2025 23rd European Control Conference (ECC)
June 24-27, 2025. Thessaloniki, Greece

Iterative Learning Control for Ramp Metering on Service Station On-ramps

Hongxi Xiang[1], Carlo Cenedese[2,3], Efe C. Balta[2,4], and John Lygeros[2]

***Abstract*— Highway congestion leads to significant delays and pollution. Regulating the outflow from the Service Station can help alleviate this congestion. Notably, traffic flows follow recurring patterns over days and weeks, allowing for the application of Iterative Learning Control (ILC). Building on these insights, we propose an ILC approach based on the Cell Transmission Model with service stations (CTM-s). It is shown that ILC can effectively compensate for potential inaccuracies in model parameter estimates by leveraging historical data.**

I. INTRODUCTION

Traffic congestion poses major environmental and economic challenges, including increased emissions, health risks, and fuel inefficiencies [1]. Since naive solutions, such as increasing capacity, are not scalable, research has focused on optimizing existing infrastructure, which requires a smaller investment and is adaptable to changing traffic conditions.

The optimal operation of highway networks has long been a focus of research due to its significant impact on overall traffic. Numerous strategies have been proposed to reduce congestion [2, 3], with on-ramp metering management emerging as one of the most effective ones [4, 5]. While on-ramp management is well-studied, the impact of Service Stations (STs) on traffic has only recently gained attention. In [6, 7], the authors proposed the "Cell Transmission Model with service stations" (CTM-s), showing that strategically placed STs can reduce the peak traffic congestion on the highway stretch. A second-order METANET-based model with an ALINEA control strategy was proposed in [8] to manage reentry flows. However, these works did not consider the repetitive nature of the traffic demand, which naturally lends itself to learning-based approaches like Iterative Learning Control (ILC).

ILC is a control strategy for iterative tasks, where the measurements of previous iterations are used for improving the control performance of subsequent iterations [9, 10]. Initially developed for unconstrained tracking, ILC was later extended to Optimization-based ILC (OB-ILC) to handle constraints [11, 12], with convergence guarantees shown in [13, 14]. Subsequent methods addressed parametric uncertainties [15, 16], iteration-varying dynamics [17], and reinforcement learning-based adaptation [18]. However, none of these methods provides robust constraint satisfaction guarantees. Recent OB-ILC frameworks [19, 20] address this gap using operator-theoretic tools to ensure constraint satisfaction under noise and model errors.

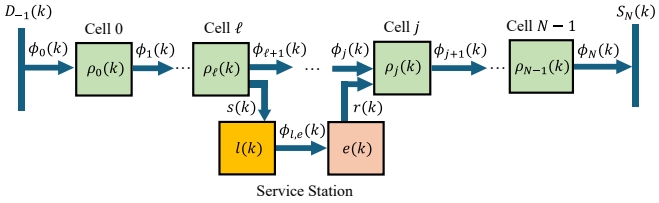

Fig. 1: Illustration of CTM-s model with one ST.

The main contributions of this paper are: (**i**) The first Model Predictive Control (MPC) based ramp metering scheme using CTM-s to control the flow exiting a ST to reduce the mainstream congestion; (**ii**) a novel ILC scheme for highway traffic control, where we systematically integrate previous traffic data into the controller design to improve performance. Our approach relaxes the knowledge and modeling requirements by providing means to compensate for parameter estimation errors. The efficacy of our ILC scheme is validated via numerical studies demonstrating convergence to the correct parameter values and performance improvement.

II. CTM-S DYNAMICS

In this section, we adapt the CTM-s model introduced in [6, 7] to our context. The time is discretized into intervals $[kT, (k+1)T)$ of length T indexed by $k \in \mathbb{N}$, and the highway stretch is divided into N consecutive cells indexed by $i \in \mathcal{N} = \{0, ..., N-1\}$, see Fig. 1. Vehicles in cell i can proceed to cell $i+1$ or exit via an off-ramp; conversely, vehicles may enter from cell $i-1$ or an on-ramp. For simplicity, we assume there is only a single ST identified by the pair (ℓ, j), where $\ell, j \in \mathcal{N}$, with ℓ and j denoting the exit and merge cells to the ST, respectively. For clarity, we focus on a highway stretch without other ramps, although the approach generalizes to more complex settings (see [6] for details).

We now present the model dynamics using the variables in Table I, separating them into linear and non-linear parts for controller design purposes.

1) Linear dynamics. The following dynamics guarantee the conservation of vehicle flows and form the cornerstone of the model. The density in cell i evolves as

$$\rho_i(k+1) = \rho_i(k) + \tfrac{T}{L_i}\left(\Phi_i^+(k) - \Phi_i^-(k)\right), \qquad (1)$$

This work was supported as a part of NCCR Automation, a National Centre of Competence in Research, funded by the Swiss National Science Foundation (grant number 51NF40_225155)
[1] Department of Mechanical and Process Engineering at ETH Zürich, Zürich, Switzerland. Email: hxiang@student.ethz.ch.
[2] Department of Information Technology and Electrical Engineering at ETH Zürich, Zürich, Switzerland. Email: lygeros@control.ee.ethz.ch.
[3] Delft Center for Systems and Control, Delft University of Technology, Delft, The Netherlands. Email: ccenedese@tudelft.nl
[4] inspire AG, Zürich, Switzerland. Email: efe.balta@inspire.ch

where the total inflow and outflow are

$$\Phi_i^+(k) = \phi_i(k) + r_i(k), \tag{2a}$$
$$\Phi_i^-(k) = \phi_{i+1}(k) + s_i(k). \tag{2b}$$

Notice that $s_i(k) = s(k) = \beta\Phi_i^-(k-1)$ if $i = \ell$ and 0 otherwise. Similarly, $r_i(k) = r(k)$ only if $i = j$ and 0 otherwise. Assume on average, vehicles spend δ time intervals (δ, T) in the service station before joining the exit queue, thus

$$l(k+1) = l(k) + T(s(k) - \phi_{l,e}(k)), \tag{3a}$$
$$e(k+1) = e(k) + T(\phi_{l,e}(k) - r(k)), \tag{3b}$$
$$\phi_{l,e}(k) = s(k-\delta). \tag{3c}$$

2) Non-linear dynamics. Nonlinearities in the model arise from flow definitions based on the minimum of upstream demand and downstream supply. The demand and supply for the cells and the ST are given by

$$D_i(k) = \min((1-\beta_i)v_i\rho_i(k), q_i^{\max}), \tag{4a}$$
$$S_i(k) = \min(w_i(\rho_i^{\max} - \rho_i(k)), q_i^{\max}), \tag{4b}$$
$$D^s(k) = \min\left(\phi_{l,e}(k) + \tfrac{e(k)}{T}, r^{\max}\right), \tag{4c}$$

where in (4a), $\beta_i = \beta$ if $i = \ell$ and $\beta_i = 0$ otherwise.

For all $i \neq j$, the flow between cell $i-1$ and i reads as

$$\phi_i(k) = \min(D_{i-1}(k), S_i(k)). \tag{5}$$

On the contrary, if $i = j$, the supply of cell i is shared by ST and cell $i-1$, so

$$\phi_i(k) = \min(D_{i-1}(k), S^{\text{ms}}(k)), \tag{6}$$

where $S^{\text{ms}}(k) := \max(S_i(k) - D^s(k)), p^{\text{ms}}S_i(k))$, this formulation replaces the use of the *middle* operator, used in [1, Eq. 3.34]. Similarly, we can compute $r(k)$ as follows

$$r(k) = \min(D^s(k), S^{\text{ST}}(k)), \tag{7}$$

where $S^{\text{ST}}(k) := \max(S_j(k) - \phi_j(k), (1-p^{\text{ms}})S_j(k))$ denotes the remaining supply of cell j available to the vehicles that aim to merge back.

As boundary conditions, we set $D_{-1}(k)$ as the exogenous upstream demand and $S_N(k) = +\infty$, hence no downstream bottleneck influences the flow on the considered stretch.

III. ST RAMP METERING

In this section, we formulate two controllers for ramp metering at the ST exit. First, an MPC based on CTM-s is formulated to optimally restrict the ST's outflow to reduce the overall congestion. Then, we augment this with an ILC scheme which exploits the repetitive nature of traffic demand.

Name	Symbol	Unit	Description
Cell parameters	L_i	[km]	Cell length
	v_i	[km/h]	Free-flow speed
	w_i	[km/h]	Congestion wave speed
	$q_i^{\max}$	[veh/h]	Flow capacity
	$\rho_i^{\max}$	[veh/km]	Jam density
ST parameters	$l^{\max}$	[veh]	Service station capacity
	$e^{\max}$	[veh]	Queue length capacity
	$r^{\max}$	[veh/h]	On-ramp capacity
	$\delta\ T$	[h]	Average time spent at ST
	β	[-]	Split ratio at cell ℓ
	p^{ms}	[-]	Priority of mainstream
Cell variables	$\rho_i(k)$	[veh/km]	Density of cell i
	$\Phi_i^+(k)$	[veh/h]	Total inflow into cell i
	$\Phi_i^-(k)$	[veh/h]	Total outflow from cell i
	$\phi_i(k)$	[veh/h]	Flow from cell $i-1$ to i
	$D_i(k)$	[veh/h]	Demand of cell i
	$S_i(k)$	[veh/h]	Supply of cell i
ST variables	$l(k)$	[veh]	Number of vehicles in ST
	$e(k)$	[veh]	Queue length
	$s(k)$	[veh/h]	Inflow to ST
	$\phi_{l,e}(k)$	[veh/h]	Flow from $l(k)$ to $e(k)$
	$D^s(k)$	[veh/h]	Demand of ST
	$r(k)$	[veh/h]	On-ramp flow from ST
Boundary conditions	$D_{-1}(k)$	[veh/h]	Initial upstream demand
	$S_N(k)$	[veh/h]	Downstream supply

TABLE I: CTM-s parameters and variables

A. MPC formulation

Ramp metering schemes based on MPC have proven effective in real-life experiments [21]. In the case of ST, the MPC controller directly influences $D^s(k)$ via the input $r_c(k)$ that controls the maximum number of vehicles that can exit the ST during the interval k. Therefore, the ST demand in (4c) under control becomes

$$D^s(k) = \min\left(\phi_{l,e}(k) + \tfrac{e(k)}{T}, r^{\max}, r_c(k)\right). \tag{8}$$

We consider a linear MPC for efficient computation and approximate the nonlinear CTM-s dynamics to attain only linear constraints.

1) Constraints. The nonlinear part of the CTM-s dynamics arises from (4)–(8). Inspired by [22], we linearize these equations by relaxation. For all $i \neq j$, we relax (5) as

$$\phi_i(k) \leqslant \min(D_{i-1}(k), S_i(k)), \tag{9}$$

where the two are equivalent if (9) is active. Substituting (4a) and (4b) into (9) leads to

$$\phi_i(k) \leqslant (1-\beta_{i-1})v_{i-1}\rho_{i-1}(k), \tag{10a}$$
$$\phi_i(k) \leqslant q_{i-1}^{\max}, \tag{10b}$$
$$\phi_i(k) \leqslant w_i(\rho_i^{\max} - \rho_i(k)), \tag{10c}$$
$$\phi_i(k) \leqslant q_i^{\max}. \tag{10d}$$

Similarly, for $i = j$ we relax (6), (7) and (8) as

$$\phi_i(k) \leqslant (1-\beta_{i-1})v_i\rho_{i-1}(k), \tag{11a}$$
$$\phi_i(k) \leqslant q_{i-1}^{\max}, \tag{11b}$$
$$r(k) \leqslant \phi_{l,e}(k) + e(k)/T, \tag{11c}$$
$$r(k) \leqslant r^{\max}, \tag{11d}$$
$$\phi_i(k) + r(k) \leqslant w_i(\rho_i^{\max} - \rho_i(k)), \tag{11e}$$
$$\phi_i(k) + r(k) \leqslant q_i^{\max}, \tag{11f}$$

where (11a) and (11b) constrain $\phi_i(k)$ by the demand of cell $i-1$, while (11c) and (11d) constrain $r(k)$ by the demand of ST. Finally, (11e) and (11f) indicate that the sum of the two is constrained by the supply of the next cell i.

Notice the approximation above ignores p^{ms}, i.e., we only consider the first terms in both $S^{\text{ms}}(k)$ and $S^{\text{ST}}(k)$. In practice, p^{ms} is usually close to 1 hence the mainstream flow has a higher priority than the flow from the ST. We promote this behavior in our controller by weighting $\phi_i(k)$ more than $r(k)$ in the cost function design, as detailed in the next section.

Among the controller's goals, we also include limiting the maximum queue length at the exit of the ST. This can be imposed via the following constraint

$$e(k) \leqslant e^{\max}, \tag{12}$$

where $e^{\max}$ is the fixed maximum queue length.

2) Cost function. The primary objective is to minimize traffic congestion on the highway stretch. We use the Total Travel Time (TTT) as the congestion metric over the whole prediction horizon, a widely used measure in highway control literature, e.g., see [1, Ch.8], defined as

$$\text{TTT}(k_0, k_0+K) := \textstyle\sum_{k=k_0}^{k_0+K}\sum_{i=0}^{N-1}\rho_i(k)L_i. \tag{13}$$

To compensate for the relaxed constraints, we design a cost function to push the variables against the constraint (10) - (11). This approach leads to optimal solutions that satisfy a subset of the constraints with equality, which, in turn, satisfy the original non-linear CTM-s dynamics. To this end, we maximize the flows $\phi_i(k)$ and $r(k)$. Therefore, the cost J minimized by the MPC becomes

$$\text{TTT}(k_0, k_0+K) - \lambda \sum_{k=k_0}^{k_0+K-1}\left(w_r r(k) + \sum_{i=0}^{N}\phi_i(k)L_{i-1}\right), \tag{14}$$

where $\lambda > 0$ and small w_r ($0 < w_r < L_{j-1}$) gives priority to the mainstream flow $\phi_j(k)$ when merging. The last term in (14) is called Total Travel Distance (TTD), see [1, Ch.8]. Since there is no cell -1, we set L_{-1} to a predefined weight. Note that during the control horizon $[k_0T, (k_0+K)T]$, the flows $\phi_i(k_0+K)$ and $r(k_0+K)$ have not taken place yet, since by definition, they are flows during $[(k_0+K)T, (k_0+K+1)T)$. Therefore, the flows are only summed up to K_0+K-1 instead of k_0+K. For the same reason, in the following section, we define $\phi_i(k)$ as part of the inputs in the MPC formulation, even though we only regulate $r(k)$, since there are no initial values to propagate the dynamics.

3) Overall formulation. To formulate linear MPC, we organize the CTM-s variables as states $x(k) := [\rho_0(k), \dots \rho_{N-1}(k), l(k), e(k)]^\top \in \mathbb{R}^{N+2}$, and inputs $u(k) := [\phi_0(k), \dots, \phi_N(k), r(k)]^\top \in \mathbb{R}^{N+2}$. Then the collection of the variables over the prediction horizon is denoted by $x_{k_0} := \text{col}\left(\{x(k_0+k)\}_{k=0}^{K}\right) \in \mathbb{R}^{(N+2)\times(K+1)}$ and $u_{k_0} := \text{col}\left(\{u(k_0+k)\}_{k=0}^{K-1}\right) \in \mathbb{R}^{(N+2)\times K}$, $\phi_{l,e,k_0} := \text{col}\left(\{\phi_{l,e}(k_0+k)\}_{k=0}^{K-1}\right) \in \mathbb{R}^{K}$.

The MPC at time at time k_0 reads as

$$\min_{u_{k_0}} J(u_{k_0}) = \tfrac{a}{2}\|x_{k_0} - x_r\|_Q^2 + c_x^\top x_{k_0} - \ c_u^\top u_{k_0}, \tag{15a}$$
$$\text{s.t.} \quad x_{k_0} = x_{\text{init},k_0} + Gu_{k_0} + G_h\ \phi_{l,e,k_0}, \tag{15b}$$
$$A_x x_{k_0} + A_u u_{k_0} \leqslant b_{k_0}, \tag{15c}$$
$$x_{k_0} \geqslant 0, u_{k_0} \geqslant 0. \tag{15d}$$

In the objective function (15a), the two linear cost terms correspond to (14). We augment the cost with an additional quadratic term to provide necessary gradient information for the ILC scheme in the next section. However, this term must be designed carefully, as it can diverge the optimal solution from satisfying the relaxed constraints (10) and (11) with equality. To minimize x, we set $x_r := 0$ in our implementation. We define a diagonal matrix $Q \succ 0$, with elements associated with $\rho_i(k)$, $l(k)$, and $e(k)$ set to $w_\rho L_i/\rho_i^{\max}$, $w_l/l^{\max}$, and $w_e/e^{\max}$, respectively, where $w_\rho, , w_l, , w_e > 0$ are normalized weights. This ensures that the quadratic terms behave approximately linearly, preserving the tightness of the optimal solution in the relaxed constraints (10) and (11) as much as possible. The predefined $a > 0$ helps to achieve a reasonable trade-off between the gradient information and the relaxation inaccuracies.

In (15b), $x_{\text{init},k_0} := \mathbb{1} \otimes x(k_0)$ with $\mathbb{1}$ as a vector of ones of the correct dimension. The constraints (1) – (3), (10) – (12) are included in compact form in (15b), (15c) and (15d), where G, G_h, A_x, A_u are matrices of the correct dimensions.

In practice, the time sampling interval T is a design choice, and highway parameters L_i, v_i, w_i, $q_i^{\max}$, $r^{\max}$ are constant and can usually be measured precisely. However, the split ratio β, average waiting time δ, and future initial demand $D_{-1}(k)$ depend on the drivers and are difficult to estimate. Therefore, (15) is solved by using the best estimates β_{es}, δ_{es}, and $D_{-1,\text{es}}(k)$ of the corresponding parameters, i.e., (15b) and (15c) are substituted by

$$x_{k_0} = x_{\text{init},k_0} + Mu_{k_0} + G_h\ \phi_{l,e,k_0,\text{es}}, \tag{16a}$$
$$A_{x,\text{es}} x_{k_0} + A_u u_{k_0} \leqslant b_{\text{es}}, \tag{16b}$$

where M, $A_{x,\text{es}}$, b_{es}, and $\phi_{l,e,k_0,\text{es}}$ are estimates of G, A_x, b, and ϕ_{l,e,k_0}, respectively, based on β_{es}, δ_{es}, and $D_{-1,\text{es}}(k)$.

After solving the MPC problem, we set the optimal input $r^*(k)$ as the control input $r_c(k)$ in (8). Although the control input is typically updated at every time step in an MPC setting, empirical experiments indicate that increasing the update interval has minimal impact on performance. In our implementation, we update the control input every p steps to reduce computational load.

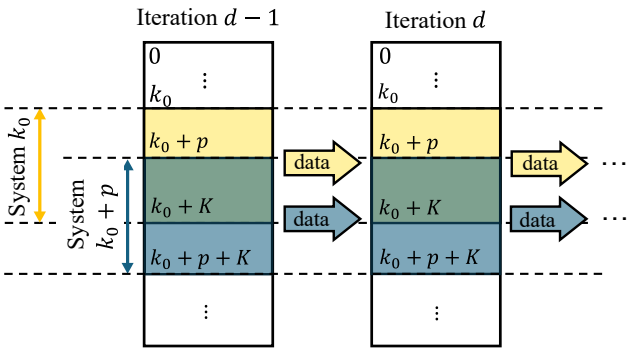

Fig. 2: General framework of applying ILC to highway traffic. Yellow and blue boxes denote *system* k_0 and *system* k_0+p (with horizon length K), respectively. We compute the control inputs for system k_0 on iteration d by (17) using data of the same system on iteration $d-1$. Then we apply the control inputs until updated at time step k_0+p for the next system.

B. ILC formulation

1) Motivation for ILC. As we will see in simulations, inaccurate estimates β_{es}, δ_{es}, and $D_{-1,\text{es}}(k)$ can significantly undermine performance. To overcome this, we leverage the repetitive nature of traffic patterns, which repeat daily and weekly, enabling us to "learn" and "improve" the estimates of the unknown parameters based on previous data.

2) The control framework. Figure 2 illustrates the implementation of ILC framework on highway traffic control. For simplicity, we assume that the traffic pattern repeats daily, though our approach can be easily adapted to any period.

We implement ILC in a receding-horizon fashion. To compute control actions at time step k_0 of iteration d (the d-th day), we use data from $k \in [k_0, k_0+K]$ collected during the previous iteration $d-1$. Control inputs are updated every p time steps, so at k_0+p, inputs are recomputed using data from $k \in [k_0+p, k_0+p+K]$ from the previous iteration. This process continues until the desired control period is covered. We refer to the traffic between k_0 and k_0+K (yellow boxes in Fig. 2) as *system* k_0, corresponding to the nominal problem (15) at k_0. Similarly, the traffic between k_0+p and k_0+p+K (blue boxes in Fig. 2) is called *system* k_0+p, and so on.

Note that we iterate horizontally rather than vertically. This is because the repetitive traffic pattern occurs across iterations (e.g., day), while the traffic during a single iteration (e.g., during one day) can vary largely at different time steps. For instance, morning peak traffic demand can differ greatly from evening demand (see Fig. 3), whereas morning peak traffic on one day is typically similar to that of previous days.

We propose an ILC formulation based on [19] and focus on a particular system k_0 and omit the subscript "k_0" if there is no ambiguity. The subscript d denotes the iteration index.

3) Formulation. Based on (15), we propose the following ILC formulation.

$$\min_{v} \ \tfrac{1}{2}\|v-u_{d-1}\|_W^2 + \alpha\, v^\top F(x_{d-1},u_{d-1}), \tag{17a}$$

$$s.t. \quad x_d = Mv + x_{\text{init},d} + x_{d-1} - Mu_{d-1} - x_{\text{init},d-1}, \tag{17b}$$

$$A_{x,es}x_d + A_u v \leqslant b_{d-1}, \tag{17c}$$

$$x_d \geqslant 0 \quad v \geqslant 0, \tag{17d}$$

where u_{d-1}, x_{d-1} are measurements from the previous iteration. b_{d-1} uses previous data $D_{-1,d-1}(k)$ and $\phi_{l,e,d-1}(k)$. In the objective (17a), $W := M^\top Q M \succ 0$ is a preconditioner matrix. Since M has full column rank, it follows that $W \succ 0$ as long as $Q \succ 0$. $\alpha > 0$ is a predefined weight and F is an approximation of the gradient of the nominal objective function (15a), defined next.

For iteration d, by replacing (15a) into (15b), we attain

$$J_d(u) = \frac{1}{2}u^\top H u + f_d^\top u + c, \tag{18}$$

where $H := a\, G^\top Q G$, $f_d := a\, G^\top Q(w_d - x_r) + G^\top c_x - c_u$, $w_d := G_h \phi_{l,e_d} + x_{\text{init,d}}$, and $c := G^\top c_x - c_u$. Then we have

$$\begin{aligned}\nabla J_d(u) &= Hu + f_d \\ &= a\,[G^\top Q(Gu + w_d - x_r)] + G^\top c_x - c_u.\end{aligned} \tag{19}$$

Since we do not know G, and w_d exactly, we define

$$F(x_{d-1},u_{d-1}) := a\,[M^\top Q(x_{d-1}-x_r)] + M^\top c_x - c_u \tag{20}$$

as an approximation of the gradient of the objective function of iteration d evaluated at input u of iteration $d-1$, as

$$\nabla J_d(u_{d-1}) = a\,[G^\top Q(Gu_{d-1} + w_d - x_r)] + G^\top c_x - c_u,$$

where we replaced the unknown G with its estimate M and $Gu_{d-1}+w_d$ by x_{d-1}. This is equivalent to replacing w_d by w_{d-1}, since $x_{d-1} = Gu_{d-1} + w_{d-1}$, according to (15b).

Next, we provide the intuition behind constraint (17b). Let $x_{d,GT}$ denote the ground truth values computed by using exact parameters, i.e., $x_{d,GT} = x_{\text{init, d}} + Gv + G_h\phi_{l,e,d}$, then the computation error when using (17b) reads as

$$\begin{aligned}\text{err}_d :=& x_{d,GT} - x_d \\ =& x_{\text{init, d}} + Gv + G_h\phi_{l,e,d} \\ & - (Mv + x_{\text{init},d} + x_{d-1} - Mu_{d-1} - x_{\text{init},d-1}) \\ =& (G-M)(v-u_{d-1}) + G_h(\phi_{l,e,d} - \phi_{l,e,d-1}),\end{aligned} \tag{21}$$

where the last equality comes from $x_{d-1} = Gu_{d-1} + x_{\text{init},d-1} + G_h\phi_{l,e,d-1}$. Therefore, since from (17a) we try to minimize the distance between v and u_{d-1}, then the estimated error $G-M$ will be compensated.

After computing (17), we apply the optimal solution $r^*(k)$ for p time intervals as $r_c(k)$, and then compute a new control input sequence by solving a new instance of (17) associated with the next system.

IV. Simulations

A. Simulations setup

We consider a highway stretch characterized by the parameters in Table III. There is a significant reduction in w_i and $q_i^{\max}$ from cell 8 to 9, creating a bottleneck. The ST is positioned upstream of this bottleneck, between cells $\ell = 4$ and $j = 6$, to mitigate traffic congestion. For details on optimal ST placement, see [7].

	$\mathbf{r}_\beta$	$\mathbf{r}_\delta$	$\mathbf{r_D}$
Underest.	0.8	0.8	0.8
Overest.	1.2	1.2	1.2

TABLE II: The scaling factors in six simulations scenarios.

The upstream demand $D_{-1}(k)$, as shown in Fig. 3, is a scaled version of the flow from the A2 highway in the Netherlands during a standard weekday, extracted from the *Nationaal Dataportaal Wegverkeer* [23]. In the simulations, $D_{-1}(k)$ is set to be constant for all days, with one iteration corresponds to one day. We focus on the morning peak from 07 : 00 to 10 : 00, denoted by t_s and t_e. We model the estimating errors of β, δ, and $D_{-1}(k)$, by the scaling factors r_β, r_δ, $r_D \geqslant 0$. Specifically, the estimated parameters are

$$\beta_\mathrm{es} = r_\beta \beta, \quad \delta_\mathrm{es} = r_\delta \delta, \quad D_{-1,\mathrm{es}}(k) = r_D D_{-1}(k), \quad (22)$$

where a scaling greater or smaller than 1 denotes an over- or underestimation of the corresponding parameter. We aim to show that over the iterations, the ILC compensates for these estimation errors, achieving performance comparable to the Ground-Truth MPC (GT-MPC), which is the MPC in (15) with the correct parameters in Table III and $D_{-1}(k)$.

B. Controllers and performance metrics

We consider six different scenarios where the parameters in (22) take values as in Table II.

Note that on the first day ($d = 0$), the ILC scheme cannot be applied due to the lack of prior data. Instead, an MPC is used with the estimates β_es, δ_es, and $D_{-1,\mathrm{es}}$.

Since our primary goal is to reduce congestion, we use $\mathrm{TTT}(t_\mathrm{s}, t_\mathrm{e})$ as main evaluation metric. The controller trade offs between alleviating congestion and maintaining a low waiting time at the ST exit. Thus, we consider two additional metrics the Total Waiting Time (TWT) and the Total Time Spent (TTS), defined as

$$\mathrm{TWT}(t_\mathrm{s}, t_\mathrm{e}) \coloneqq \sum_{k=t_\mathrm{s}}^{t_\mathrm{e}} e(k), \quad (23a)$$

$$\mathrm{TTS}(t_\mathrm{s}, t_\mathrm{e}) \coloneqq \mathrm{TTT}(t_\mathrm{s}, t_\mathrm{e}) + \mathrm{TWT}(t_\mathrm{s}, t_\mathrm{e}). \quad (23b)$$

TWT measures the waiting time at the ST exit, while TTS represents the overall time for traveling and waiting.

To better assess the convergence performance of ILC to GT-MPC, we define the following relative indices, where the superscript indicates the controller used,

$$\Delta_\mathrm{TTT} \coloneqq \mathrm{TTT}^\mathrm{ILC}(t_\mathrm{s}, t_\mathrm{e}) - \mathrm{TTT}^\mathrm{GT-MPC}(t_\mathrm{s}, t_\mathrm{e}), \quad (24a)$$

$$\Delta_\mathrm{TWT} \coloneqq \mathrm{TWT}^\mathrm{ILC}(t_\mathrm{s}, t_\mathrm{e}) - \mathrm{TWT}^\mathrm{GT-MPC}(t_\mathrm{s}, t_\mathrm{e}), \quad (24b)$$

$$\Delta_\mathrm{TTS} \coloneqq \mathrm{TTS}^\mathrm{ILC}(t_\mathrm{s}, t_\mathrm{e}) - \mathrm{TTS}^\mathrm{GT-MPC}(t_\mathrm{s}, t_\mathrm{e}), \quad (24c)$$

Finally, we define the maximum rate of violating the queue length constraint (12) over $[t_s, t_e]$ as

$$\Delta_{e^\mathrm{max}}(t_\mathrm{s}, t_\mathrm{e}) \coloneqq \max_{k \in [t_\mathrm{s}, t_\mathrm{e}]} \left(\frac{\max\left(e(k) - e^\mathrm{max}, 0\right)}{e^\mathrm{max}} \right). \quad (25)$$

If there is never a violation, then $\Delta_{e^\mathrm{max}} = 0$.

	i	L_i	v_i	w_i	q_i^max	ρ_max^i
Cells	0	0.65	103	31	1870	79
	1	0.56	103	25	1735	86
	2	0.61	103	33	1876	75
	3	0.23	103	26	1757	84
	4	0.34	103	33	1780	71
	5	0.54	103	35	1847	71
	6	0.29	103	38	1985	72
	7	0.31	103	40	2092	73
	8	0.59	103	40	2002	69
	9	0.6	96	29	1714	77
	10	0.41	96	29	1705	76
	11	0.2	103	33	1845	74
	12	0.7	103	35	1924	74
	13	0.53	104	30	1774	77
	14	0.51	103	27	1789	83
ST	l^max	e^max	r^max	δ	β	p^ms
	400	20	1500	480	0.1	0.9
Other	T [s]	K	p	λ	a	α
	10	90	30	0.5	1	1
	w_ρ	w_e	w_l	w_r	L_{-1}	
	1	0.1	0.05	0.1	0.5	

TABLE III: Parameters used in the simulations.

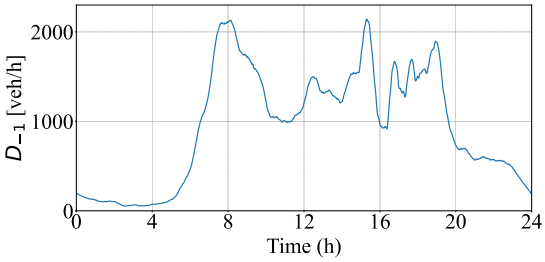

Fig. 3: Initial upstream demand $D_{-1}(k)$.

C. Results

Table IV presents results for the highway without control and under GT-MPC. Notably, TTS are almost equal in both cases, reflecting the expected trade-off between TTT and TTS. With its precise parameter knowledge, GT-MPC effectively reduces congestion (lower TTT) while maintaining $\Delta_{e^\mathrm{max}} = 0$.

Figure 4 shows the relative performance of ILC across six scenarios summarized in Table II. The first three sub-figures are on a logarithmic scale. At iteration 0, MPC using wrongly estimated parameters results in positive values of Δ_TTT, suggesting that imprecise parameter knowledge undermines congestion reduction. In some cases, such as underestimating β, the controller can yield both positive Δ_TTT and Δ_TWT, increasing overall TTS and potentially violating queue length constraints. Remarkably, by leveraging previous data, ILC converges rapidly to GT-MPC (within one or two iterations), achieving lower Δ_TTT (and thus lower TTT), as indicated by the fast convergence of all curves to a neighborhood of 0 value. Additionally, the queue length constraint is consistently

	TTT	TWT	TTS	$\Delta_{e^{\max}}$
Uncontrolled	358.49	0.55	359.04	0
GT-MPC	344.64	14.63	359.27	0

TABLE IV: Performance of uncontrolled stretch and the one under GT-MPC.

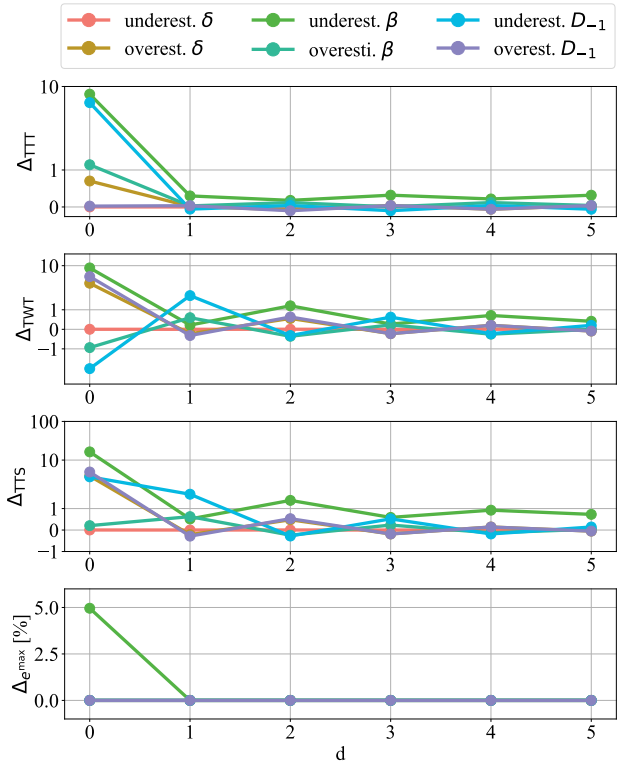

Fig. 4: Relative performance of the ILC scheme over 5 iterations with the scenarios in Table II.

satisfied, demonstrating the effectiveness of our ILC approach.

V. CONCLUSIONS

ILC tailored to CTM-s model is an effective algorithm for highway traffic control, mitigating parameter estimating errors. Numerical experiments demonstrate that by leveraging repetitive traffic patterns, our ILC approach quickly converges to GT-MPC, recovering from incorrect initial estimates and outperforms MPC under the same conditions, even when estimated values differ by 20% from the correct ones.

This study focuses on a single highway with one service station. An interesting extension is to apply this approach to more complex road networks with multiple stations, where coordinated control may yield better performance. Another potential direction is developing a nonlinear ILC to address model mismatch introduced by the linear relaxation of the CTM-s model. Our current formulation requires an extra cost term TTD, which can potentially diverge the controller from the original goal of reducing TTT. With a non-linear formulation, we might skip relaxation and remove TTD, and therefore reduce congestion more effectively.

REFERENCES

[1] A. Ferrara, S. Sacone, S. Siri, *et al.*, *Freeway traffic modelling and control*, vol. 585. Springer, 2018.

[2] M. Papageorgiou, C. Diakaki, V. Dinopoulou, A. Kotsialos, and Y. Wang, "Review of road traffic control strategies," *Proceedings of the IEEE*, vol. 91, no. 12, pp. 2043–2067, 2003.

[3] I. Papamichail, M. Papageorgiou, and Y. Wang, "Motorway traffic surveillance and control," *European Journal of Control*, vol. 13, no. 2-3, pp. 297–319, 2007.

[4] M. Papageorgiou and A. Kotsialos, "Freeway ramp metering: An overview," *IEEE transactions on intelligent transportation systems*, vol. 3, no. 4, pp. 271–281, 2002.

[5] F. Vrbanić, E. Ivanjko, K. Kušić, and D. Čakija, "Variable speed limit and ramp metering for mixed traffic flows: A review and open questions," *Applied Sciences*, vol. 11, no. 6, p. 2574, 2021.

[6] C. Cenedese, M. Cucuzzella, A. Ferrara, and J. Lygeros, "A novel control-oriented cell transmission model including service stations on highways," in *2022 IEEE 61st Conference on Decision and Control (CDC)*, pp. 6278–6283, IEEE, 2022.

[7] C. Cenedese, M. Cucuzzella, A. C. Ramusino, D. Spalenza, J. Lygeros, and A. Ferrara, "Optimal service station design for traffic mitigation via genetic algorithm and neural network," *IFAC-PapersOnLine*, vol. 56, no. 2, pp. 1528–1533, 2023.

[8] A. Kamalifar, C. Cenedese, M. Cucuzzella, and A. Ferrara, "A new control-oriented METANET model to encompass service stations on highways," in *2024 European Control Conference (ECC)*, pp. 1387–1392, 2024.

[9] M. Uchiyama, "Formation of high-speed motion pattern of a mechanical arm by trial," *Transactions of the Society of Instrument and Control Engineers*, vol. 14, no. 6, pp. 706–712, 1978.

[10] S. Arimoto, S. Kawamura, and F. Miyazaki, "Bettering operation of robots by learning," *Journal of Robotic systems*, vol. 1, no. 2, pp. 123–140, 1984.

[11] S. Mishra, U. Topcu, and M. Tomizuka, "Optimization-based constrained iterative learning control," *IEEE Transactions on Control Systems Technology*, vol. 19, no. 6, pp. 1613–1621, 2010.

[12] D. H. Owens and J. Hätönen, "Iterative learning control—an optimization paradigm," *Annual reviews in control*, vol. 29, no. 1, pp. 57–70, 2005.

[13] N. Amann, D. H. Owens, and E. Rogers, "Iterative learning control for discrete-time systems with exponential rate of convergence," *IEE Proceedings-Control Theory and Applications*, vol. 143, no. 2, pp. 217–224, 1996.

[14] A. Schöllig and R. D'Andrea, "Optimization-based iterative learning control for trajectory tracking," in *2009 European Control Conference (ECC)*, pp. 1505–1510, IEEE, 2009.

[15] Q. Yu and Z. Hou, "Data-driven predictive iterative learning control for a class of multiple-input and multiple-output nonlinear systems," *Transactions of the Institute of Measurement and Control*, vol. 38, no. 3, pp. 266–281, 2016.

[16] S.-K. Oh and J. M. Lee, "Stochastic iterative learning control for discrete linear time-invariant system with batch-varying reference trajectories," *Journal of Process Control*, vol. 36, pp. 64–78, 2015.

[17] D. Meng and K. L. Moore, "Robust iterative learning control for nonrepetitive uncertain systems," *IEEE Transactions on Automatic Control*, vol. 62, no. 2, pp. 907–913, 2016.

[18] B. Nemec, M. Simonič, N. Likar, and A. Ude, "Enhancing the performance of adaptive iterative learning control with reinforcement learning," in *2017 IEEE/RSJ international conference on intelligent robots and systems (IROS)*, pp. 2192–2199, IEEE, 2017.

[19] D. Liao-McPherson, E. C. Balta, A. Rupenyan, and J. Lygeros, "On robustness in optimization-based constrained iterative learning control," *IEEE Control Systems Letters*, vol. 6, pp. 2846–2851, 2022.

[20] E. C. Balta, D. M. Tilbury, and K. Barton, "Iterative learning spatial height control for layerwise processes," *Automatica*, vol. 167, p. 111756, 2024.

[21] T. Bellemans, B. De Schutter, and B. De Moor, "Model predictive control for ramp metering of motorway traffic: A case study," *Control Engineering Practice*, vol. 14, no. 7, pp. 757–767, 2006.

[22] G. Gomes and R. Horowitz, "Optimal freeway ramp metering using the asymmetric cell transmission model," *Transportation Research Part C: Emerging Technologies*, vol. 14, no. 4, pp. 244–262, 2006.

[23] Nationaal Dataportaal Wegverkeer, "DEXTER Data Exploration + Exporter." https://dexter.ndw.nu/. Accessed: 2024.